

PI3K(p110 α) Protects Against Myocardial Infarction-Induced Heart Failure

Identification of PI3K-Regulated miRNA and mRNA

Ruby C.Y. Lin, Kate L. Weeks, Xiao-Ming Gao, Rohan B.H. Williams, Bianca C. Bernardo, Helen Kiriazis, Vance B. Matthews, Elizabeth A. Woodcock, Russell D. Bouwman, Janelle P. Mollica, Helen J. Speirs, Ian W. Dawes, Roger J. Daly, Tetsuo Shioi, Seigo Izumo, Mark A. Febbraio, Xiao-Jun Du, Julie R. McMullen

Objective—Myocardial infarction (MI) is a serious complication of atherosclerosis associated with increasing mortality attributable to heart failure. Activation of phosphoinositide 3-kinase [PI3K(p110 α)] is considered a new strategy for the treatment of heart failure. However, whether PI3K(p110 α) provides protection in a setting of MI is unknown, and PI3K(p110 α) is difficult to target because it has multiple actions in numerous cell types. The goal of this study was to assess whether PI3K(p110 α) is beneficial in a setting of MI and, if so, to identify cardiac-selective microRNA and mRNA that mediate the protective properties of PI3K(p110 α).

Methods and Results—Cardiomyocyte-specific transgenic mice with increased or decreased PI3K(p110 α) activity (caPI3K-Tg and dnPI3K-Tg, respectively) were subjected to MI for 8 weeks. The caPI3K-Tg subjected to MI had better cardiac function than nontransgenic mice, whereas dnPI3K-Tg had worse function. Using microarray analysis, we identified PI3K-regulated miRNA and mRNA that were correlated with cardiac function, including growth factor receptor-bound 14. Growth factor receptor-bound 14 is highly expressed in the heart and positively correlated with PI3K(p110 α) activity and cardiac function. Mice deficient in growth factor receptor-bound 14 have cardiac dysfunction.

Conclusion—Activation of PI3K(p110 α) protects the heart against MI-induced heart failure. Cardiac-selective targets that mediate the protective effects of PI3K(p110 α) represent new drug targets for heart failure. (*Arterioscler Thromb Vasc Biol.* 2010;30:724-732.)

The most common cause of heart failure is atherosclerotic coronary artery disease. Coronary artery occlusion leads to myocardial infarction (MI), which causes necrosis to an area of the myocardium, pathological remodeling (cardiac hypertrophy, cell death, and fibrosis), and cardiac dysfunction. Postinfarction heart failure is associated with high morbidity and mortality rates and has increased in prevalence because of less mortality associated with acute coronary events with improved reperfusion therapies. In general, therapeutics and research have focused on inhibiting pathological processes that contribute to heart failure. We previously reported the potential of a proactive intervention via activation of the insulin-like growth factor-1–phosphoinositide 3-kinase (PI3K, p110 α) pathway in mouse models of pressure overload or dilated cardiomyopathy.^{1–3} Increased PI3K activity improved either lifespan or cardiac function in these

models. The protective effect of the insulin-like growth factor-1–PI3K pathway relates to its critical role in regulating physiological growth of the heart (eg, postnatal developmental growth or exercise-induced growth). In contrast with pathological heart growth/hypertrophy, physiological growth is not associated with fibrosis, dysfunction, or increased morbidity and mortality.^{4–6} It is now generally accepted that the insulin-like growth factor-1–PI3K(p110 α) pathway regulates physiological hypertrophy and cardiac protection, whereas activation of other signaling cascades, including those downstream of G-protein-coupled receptors, regulate pathological hypertrophy.⁶ The aim of the current study was to examine whether PI3K is beneficial in a setting of MI-induced heart failure and, if so, to identify PI3K-regulated targets that mediate its protective properties. Whereas growing evidence shows the benefits of activating the insulin-like

Received on: August 10, 2009; final version accepted on: January 13, 2010.

From Ramaciotti Centre for Gene Function Analysis (R.C.Y.L., H.J.S., I.W.D.), University of New South Wales, Randwick, Australia; Baker IDI Heart and Diabetes Institute (K.L.W., X.-M.G., B.C.B., H.K., V.B.M., E.A.W., R.D.B., J.P.M., M.A.F., X.-J.D., J.R.M.), Melbourne, Australia; Department of Biochemistry and Molecular Biology (K.L.W.), University of Melbourne, Victoria, Australia; Molecular Systems Biology Group (R.B.H.W.), John Curtin School of Medical Research, Australian National University, Canberra City, Australia; Cancer Research Program (R.J.D.), Garvan Institute of Medical Research, Sydney, Australia; St. Vincent's Hospital Clinical School (R.J.D.), University of New South Wales, Sydney, Australia; Beth Israel Deaconess Medical Center & Harvard Medical School (T.S., S.I.), Boston, Mass.

R.C.Y.L. and K.L.W. contributed equally to this manuscript.

Correspondence to Julie R. McMullen, Baker IDI Heart and Diabetes Institute, PO Box 6492 St. Kilda Road Central, Melbourne, Victoria 8008, Australia. E-mail Julie.mcmullen@bakeridi.edu.au

© 2010 American Heart Association, Inc.

Arterioscler Thromb Vasc Biol is available at <http://atvb.ahajournals.org>

DOI: 10.1161/ATVBAHA.109.201988

growth factor-1–PI3K pathway in the heart,⁷ there are challenges in targeting PI3K(p110 α) directly because of the numerous actions of PI3K(p110 α) in various cell types. Therefore, we set out to identify cardiac-selective miRNA and mRNA regulated by PI3K(p110 α) in a setting of cardiac stress that would represent better drug targets.

Materials and Methods

Experimental Animals

The Alfred Medical Research and Education Precinct Animal Ethics Committee approved animal care and experimentation. Mice originated from the laboratory of Dr. Seigo Izumo (Beth Israel Deaconess Medical Center and Harvard Medical School). Cardiomyocyte-specific transgenic (Tg) mice (FVB/N background) with increased PI3K(p110 α) activity (constitutively active PI3K(p110 α) [caPI3K]) or decreased PI3K(p110 α) activity (dominant-negative PI3K(p110 α) [dnPI3K]) were generated as described.⁸ The caPI3K-Tg have elevated cardiac PI3K(p110 α) activity and hearts that are 20% larger with normal cardiac function (physiological hypertrophy, “athlete’s heart”).⁸ By contrast, dnPI3K-Tg have decreased cardiac PI3K(p110 α) activity and hearts that are 20% smaller than those of nontransgenic (Ntg) littermates.⁸

Growth receptor-bound (Grb) 14 knockout (KO) mice (C57BL/6 background) and controls (wild-type [WT]; heterozygotes [Grb14^{+/-}]) were previously generated as described.⁹ These mice originated from the laboratory of Professor Roger Daly (Garvan Institute of Medical Research).

Experimental Protocols

The most widely used mouse models for atherosclerosis do not usually exhibit MI; thus, in this study, we used a surgical model of MI. At 3 to 4 months of age, PI3K and Ntg mice were subjected to MI or the sham surgery for 8 weeks as described.¹⁰ In brief, open-chest surgery was performed for permanent occlusion of the left coronary artery or sham operation. Infarcted and noninfarcted left ventricle (LV) endocardial surface areas were measured from digital images of the LV pinned flat. Infarct size was calculated as a percentage of the infarct area over the entire LV area, as described.¹¹ A subset of Grb14 KO and controls (WT, Grb14^{+/-}) were subjected to MI for 6 weeks.

Echocardiography

Transthoracic echocardiography was performed using a Hewlett Packard Sonos 5500 with a 15-MHz linear array transducer in anesthetized mice (2,2,2-tribromoethanol:240 mg/kg, intraperitoneal). LV wall thicknesses, LV chamber dimensions, fractional shortening (FS), and heart rate were determined from M-mode tracings.

Hemodynamics

Arterial pressures, LV systolic and diastolic pressures, maximal rates of increase and decrease of LV pressures (dP/dt_{max}, dP/dt_{min}), and heart rate were measured in anesthetized mice (ketamine/xylazine/atropine, 100/10/1.2 mg/kg, intraperitoneal) using a 1.4-Fr Millar MIKRO-TIP catheter and a Powerlab System (ADInstruments) as described.¹²

Protein Analysis

Lysates from heart tissue or isolated adult cardiac myocytes¹ were prepared as described¹³ for assessment of pAkt, Grb14, and brain-derived neurotrophic factor (BDNF) by Western blotting. A detailed description is presented in the Supplemental Materials (available at <http://atvb.ahajournals.org>).

AMP-Activated Protein Kinase Activity Assay

AMP-activated protein kinase (AMPK) activity was assessed in heart lysates from adult Ntg and caPI3K-Tg mice as described.¹⁴

Microarray Studies

A detailed description is presented in the Supplemental Materials. In brief, total RNA was extracted from the noninfarcted myocardium using TRIzol Reagent (Invitrogen). Differentially expressed mRNA and miRNA were then identified in the 6 models (ie, Ntg sham, dnPI3K sham, caPI3K sham, Ntg MI, dnPI3K MI, and caPI3K MI), followed by analysis to examine whether expression correlated with cardiac function (ie, FS). Finally, genes that were specifically or selectively expressed in cardiac muscle were identified using a bioinformatics approach.

Statistical Analysis

Results are presented as mean \pm SE. Differences between the groups were compared using 1-way ANOVA followed by the Fisher protected least-significant difference or Tukey post hoc test. A value of $P < 0.05$ was considered significant.

Results

PI3K(p110 α) Is Protective in a Model of MI

Cardiac function was assessed in adult PI3K-Tg and Ntg littermate controls 8 weeks after MI or the sham operation. Because the aim of the study was to assess the effect of PI3K in viable myocardium, we selected mice with similar infarct sizes of $\approx 30\%$ (Ntg, 30.4% \pm 0.9%, n=11; dnPI3K, 29.3% \pm 0.6%, n=9; caPI3K, 30.1% \pm 0.9%, n=11). Cardiac function was decreased in control animals (Ntg) after 8 weeks of MI compared with Ntg sham (Table 1, see FS). Cardiac function declined more in dnPI3K MI than in Ntg MI mice. By contrast, the decrease in FS was less in caPI3K-Tg subjected to MI for 8 weeks in comparison to Ntg MI subjected to MI (Table 1, see FS). These changes in cardiac function were largely attributable to a significant increase in the chamber dimensions of dnPI3K-Tg after MI and a trend for a reduction in LV end-systolic dimension in caPI3K-Tg (Table 1). Cardiac function was also assessed by measurement of hemodynamic parameters. MI led to a decrease in arterial blood pressure, LV systolic pressure, and maximum rates of increase or decrease in LV pressure (dP/dt_{max} and dP/dt_{min}; Table 1). The caPI3K-Tg had better cardiac contractility after MI than Ntg or dnPI3K-Tg (dP/dt_{max} in Table 1). Together, this indicates that PI3K(p110 α) is important for maintaining cardiac function in a setting of cardiac stress and that elevated levels of PI3K(p110 α) are beneficial.

Combining Genetic Profiling With Cardiac Function From PI3K-Tg Mouse Models to Identify Biologically Relevant Candidate Genes Regulated by PI3K(p110 α)

To identify PI3K-regulated targets, we performed microarray analysis on hearts of caPI3K-Tg, dnPI3K-Tg, and Ntg littermates. Under basal conditions, cardiac function (as assessed by FS) is similar in PI3K-Tg (ca and dn) and Ntg mice.^{1,3,8} Because we set out to identify genes that were correlated with cardiac function, we subjected adult Ntg or PI3K-Tg mice to a cardiac stress, ie, MI. This represented a powerful approach to identify PI3K-regulated genes that are likely to have a functional role, because the decrease in cardiac function (ie, FS) in response to MI was genotype-dependent (dnPI3K-Tg, poor cardiac function; caPI3K-Tg, improved cardiac function compared to Ntg; Table 1). From a total of 3212 genes differentially expressed between the 6 groups (Ntg sham, Ntg

Table 1. Cardiac Dimension, Function, and Morphometrics of Ntg and PI3K Tg Mice Subjected to MI or Sham Operation

	Ntg Sham	Ntg MI	dnPI3K Sham	dnPI3K MI	caPI3K Sham	caPI3K MI
	N=16–17	N=11–12	N=11	N=9	N=10	N=11
Echocardiography						
HR, bpm	512±11	516±12	480±24	454±19	525±18	498±12
Infarct area, %	0	30.4±0.9*	0	29.3±0.6*	0	30.1±0.9*
LVEDd, mm	3.64±0.09	4.72±0.14*	3.59±0.11	4.63±0.20*	3.87±0.09	4.54±0.16*
LVESd, mm	1.74±0.07	2.77±0.17*	1.65±0.07	2.99±0.24*	1.76±0.11	2.42±0.13*†
LVPW, mm	0.75±0.03	0.66±0.03	0.62±0.04‡	0.55±0.03	0.88±0.05‡	0.71±0.05*†
IVS, mm	0.82±0.05	0.68±0.07*	0.65±0.04‡	0.58±0.04	1.04±0.04‡	0.81±0.06*†
FS, %	52±1	42±2§	54±1	36±3§	54±2	47±1*†
	N=12	N=11	N=11	N=7	N=9	N=9
Catheterization						
HR, bpm	349±9	333±12	344±13	345±14	330±10	357±9
SBP, mm Hg	116±3	93±4*	104±5	89±5*	110±6	95±4*
DBP, mm Hg	78±3	70±2	74±3	68±4	71±4	72±3
LVSP, mm Hg	114±3	92±3*	101±4	87±4*‡	110±5	96±4*
LVDP, mm Hg	4±1	2±1	2±0	3±1	3±0	2±0
dP/dt _{max} , mm Hg/sec	7895±288	5458±233*	6624±173‡	4762±137*	8674±530¶	6376±229*†
dP/dt _{min} , mm Hg/sec	6957±292	3684±170*	5732±313‡	3634±177*	6714±441¶	4127±163*
	N=16–17	N=11–12	N=11	N=9	N=10	N=11
Morphometrics						
Body weight, grams	32.9±1.3	33.0±1.5	32.5±2.2	29.6±1.8	32.9±1.3	31.6±1.5
Tibial length, mm	17.0±0.1	17.1±0.1	17.1±0.1	16.9±0.2	17.1±0.1	17.2±0.1
LV weight, mg	86.8±4.4	105.9±4.9* (9)	67.4±3.8‡	80.1±4.2	114.6±4.0‡	111.4±4.9

(P=0.06 vs dnPI3K)

DBP indicates diastolic blood pressure; dP/dt_{max} and dP/dt_{min}, maximum rate of increase and decrease of LV pressures; HR, heart rate; IVS, interventricular septum thickness at diastole; LVEDd, LV end-diastolic dimensions at diastole; LVESd, LV end-systolic dimensions at diastole; LVPW, LV posterior wall thickness at diastole; LVSP, LV systolic pressure; LVDP, LV diastolic pressure; SBP, systolic blood pressure.

*P<0.05 vs sham of the same group.

†P<0.05 vs dnPI3K MI.

‡P<0.06 vs Ntg sham.

§P<0.001 vs sham of the same group.

¶P<0.05 vs dnPI3K sham.

||P<0.05 vs Ntg MI.

MI, dnPI3K sham, dnPI3K MI, caPI3K sham, caPI3K MI; Supplemental Figure I heat map and Supplemental Table IA, IB, available at <http://atvb.ahajournals.org>, 295 genes were correlated directly with FS across the 6 models (Supplemental Table II). Gene ontology (GO) analysis demonstrated a significant enrichment in genes involved in mitochondrial physiology, specifically oxidoreductase activity (GO: 0016491, with 20% of 295 vs 6% of all genes); mitochondrial inner membrane (GO: 0005743; 9% vs 2% of all genes); and electron transport (GO: 0006118; 10% vs 3% of all genes). The GO term “lipid metabolic process” (GO: 0006629) was also significantly enriched (13% of 295 vs 5% of all genes). Other sets of enriched genes in the 295 data set included a cluster of potassium voltage-gated channels (*Kcnd2*, *Kcnv2*, *Kcnt2*, and *Kcnh2*: all positively correlated with FS, except *Kcnt2*, which was negatively correlated), a cluster of 2 crystallin superfamily genes (crystallin beta A4 and crystallin beta B3) positively correlated with FS, and a cluster of histone genes

(*H2afv*, *Hist1h4h*, *Hist2h2aa1*, *Hist1h3a*) positively correlated with FS.

Finally, to identify more specific candidate genes from those differentially regulated in the PI3K models and correlated with cardiac function (ie, genes presented in Table II), we identified genes that were specifically or selectively expressed in cardiac muscle. By restricting these genes to those with >25% of expression attributable to heart tissue, we identified the following set of candidate genes: *Acadm* (medium chain acyl-Coenzyme A dehydrogenase), *Grb14*, and *Asb15* (ankyrin repeat and SOCS box-containing protein 15).

Grb14 Protects the Heart Against Cardiac Dysfunction

Grb14 gene expression was positively correlated with cardiac function (Table II) and was of particular interest because it is highly expressed in the mouse heart in comparison with other tissues.⁹ Consistent with our mRNA data, Grb14 protein

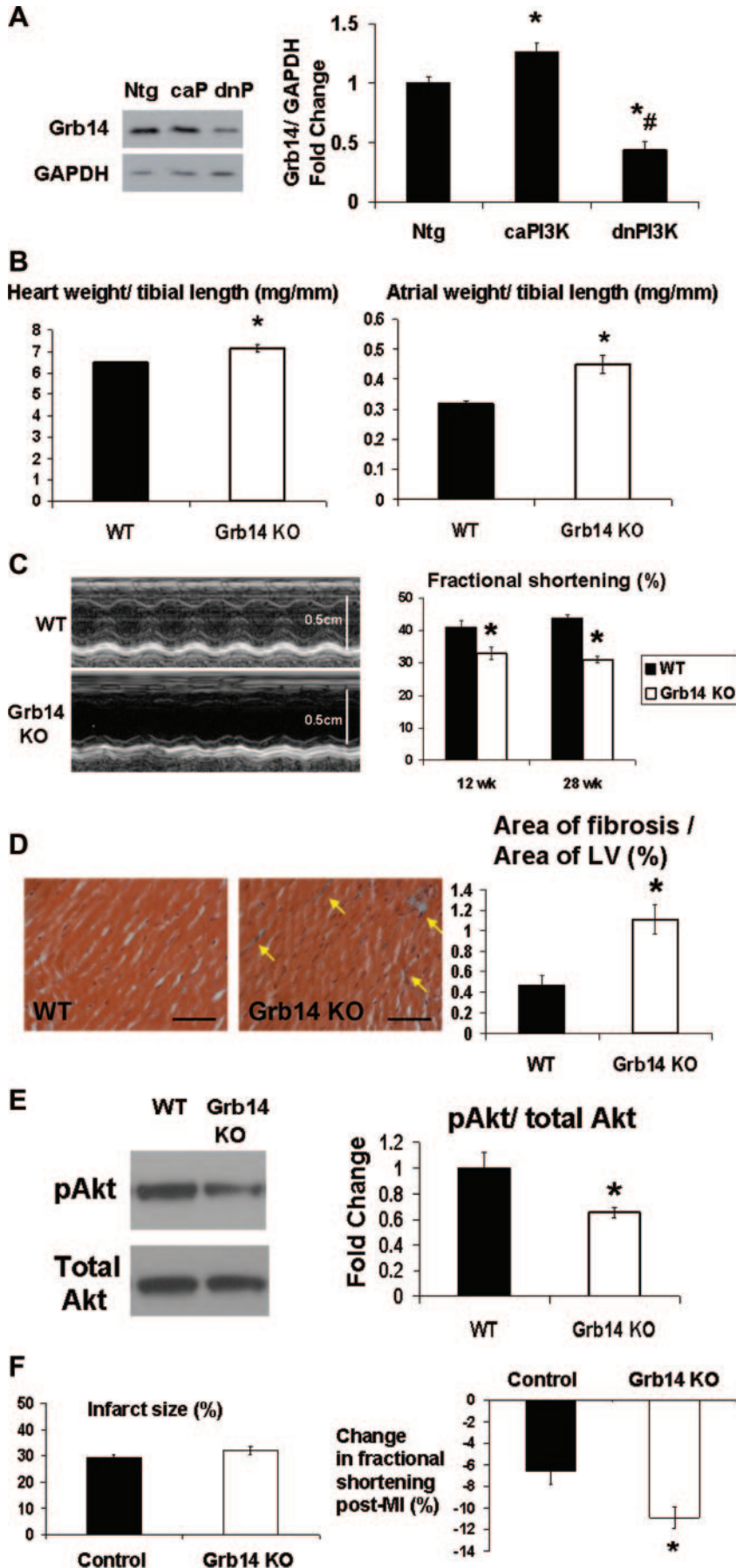


Figure 1. Grb14 protects the heart against cardiac dysfunction. **A**, Western blot of Grb14 and GAPDH expression (left) in hearts from adult Ntg, caPI3K (caP), and dnPI3K (dnP) mice. Right, Quantitative analysis of Grb14 normalized to GAPDH. Mean values for Ntg were normalized to 1; n=3–4 in each group. * P <0.05 vs Ntg. # P <0.05 vs caPI3K. **B**, Heart weight/tibial length and atrial weight/tibial length ratios in WT (n=3) and Grb14 KO mice (n=6) at age 28 weeks. **C**, Representative echocardiographic measurements (M-mode) of hearts from a WT and a Grb14 KO mouse at 28 weeks (left). Right, FS (%) at 12 weeks and 28 weeks in Grb14 KO mice (12 weeks, n=11; 28 weeks, n=7) compared with WT mice (12 weeks, n=8; 28 weeks, n=5). * P <0.05 vs WT. **D**, Representative sections from the LV wall of WT and Grb14 KO mice (left). Interstitial fibrosis appears blue on Masson trichrome stain (yellow arrows). Original magnification \times 400, scale bar=50 μ m. Right, Quantitation of the area of fibrosis/area of LV (WT, n=5; Grb14 KO, n=6). * P <0.05 vs WT. **E**, Western blot of pAkt and total Akt in hearts from adult mice (left). Right, Quantitative analysis of pAkt relative to total Akt. Mean values for Ntg were normalized to 1, n=3 in each group. * P <0.05 vs WT. **F**, Infarct size (left) relative to the LV in Grb14 KO and control mice (WT or Grb14^{+/-}) at \approx 30 weeks of age (6 weeks after infarct). Right, change in FS (%) before MI and 6 weeks after MI in Grb14 KO (n=4) and control mice (n=3). * P <0.05 vs control.

Table 2. Echocardiographic Analysis of Heart Dimensions and Function of Grb14 KO Mice at Age 28 Weeks

	WT	Grb14 KO
N of animals	5	7
HR, bpm	575±6	546±11
IVS, mm	0.82±0.08	0.69±0.05
LVPW, mm	0.67±0.09	0.63±0.04
LVEDd, mm	3.35±0.13	3.90±0.11*
LVESd, mm	1.92±0.12	2.71±0.09*
FS, %	43±1	31±1*

* $P < 0.05$ compared to WT.

expression was higher in hearts of caPI3K mice and was significantly lower in hearts of dnPI3K mice (Figure 1A). Grb14 KO mice were previously generated, with both males and females reported to display a reduction in body weight of 5% to 10% compared with WT controls; however, interestingly, this was associated with an increase in heart weight (cardiac function not assessed; other organ weights were decreased or unchanged).⁹ Consistent with the earlier report, heart weight/tibial length was increased in Grb14 KO mice compared with WT mice in the current study (Figure 1B). Ventricular weight/tibial length and atrial weight/tibial length were also higher in Grb14 KO mice vs WT mice (atrial weight; Figure 1B; ventricular weight/tibial length, 6.7 ± 0.1 vs 6.2 ± 0.1 mg/mm in Grb14 KO and WT mice, respectively; $P < 0.05$). By echocardiography, LV systolic function (FS) was decreased by $\approx 25\%$ in Grb14 KO mice at 12 and 28 weeks of age compared with WT controls (Figure 1C). The decline in FS was largely attributable to a significant increase in LV end-systolic dimension (Table 2). On histological analysis, collagen deposition was higher in ventricular sections from Grb14 KO mice compared with WT mice at 28 weeks (Figure 1D). Phosphorylation of Akt (downstream target of PI3K) was decreased in hearts of Grb14 KO mice in comparison with hearts from WT mice (Figure 1E). Finally, to assess whether Grb14 KO animals were more susceptible

to a cardiac insult (as observed in dnPI3K-Tg mice), we subjected a subset of Grb14 KO mice to MI for 6 weeks. The decline in systolic function (ie, change in FS from pre-MI values) was exacerbated in Grb14 KO mice relative to control mice (WT or Grb14^{+/-}) in response to MI; infarct sizes between the groups were not different (Figure 1F). Together, these data indicate that loss of Grb14 has an adverse impact on the heart, and decreased expression of Grb14 in the dnPI3K heart is likely to contribute to cardiac dysfunction in dnPI3K mice subjected to MI. The biological role of Grb14 in the heart also demonstrates the potential of identifying candidate genes by combining a microarray and functional approach.

Identification of PI3K(p110 α)-Regulated miRNA Associated With Cardiac Protection

The miRNA differentially expressed in the 6 groups are presented in a heat map (Figure 2, Table III). To identify miRNA that are likely to play a distinct role in regulating physiological heart growth, we first selected those miRNA that were differentially expressed in the dnPI3K-Tg and caPI3K-Tg mouse models (sham-operated mice vs Ntg sham). The miRNA that were decreased in hearts of caPI3K-Tg and increased in hearts of dnPI3K-Tg are presented in a Table with predicted mRNA targets (Table IV; predictions based on the presence of conserved seed sequences within the mRNA that complement the miRNA). We then selected those miRNA that were differentially regulated in a setting of physiological hypertrophy and cardiac protection (caPI3K sham model) and cardiac stress (Ntg MI). Differentially expressed miRNA along with predicted targets are presented in Figure 2. Three miRNA (miRNA-222, miRNA-34a, and miRNA-210) were of particular interest because they were differentially regulated in hearts of caPI3K sham and dnPI3K sham, increased in Ntg MI vs caPI3K sham/Ntg sham, and expression was greatest in dnPI3K MI mice (Figure 3A). Interestingly, miRNA-222, miRNA-34a and miRNA-210 were also highly inversely correlated with *Grb14* gene expression (Figure 3B; $P < 0.001$).

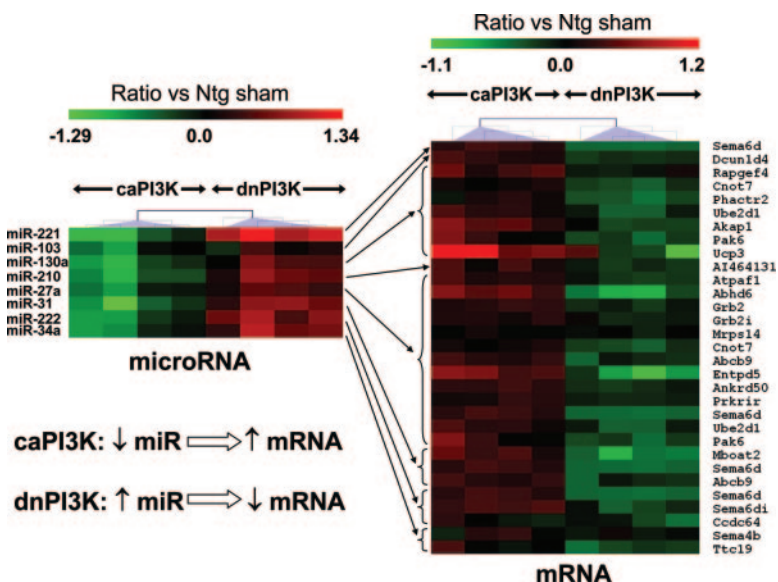


Figure 2. The miRNA differentially regulated in hearts with increased PI3K activity (caPI3K sham) or decreased PI3K activity (dnPI3K sham) and predicted mRNA targets. Each row represents a gene and each column represents an individual heart sample. Red represents upregulation in comparison to Ntg sham and green represents downregulation.

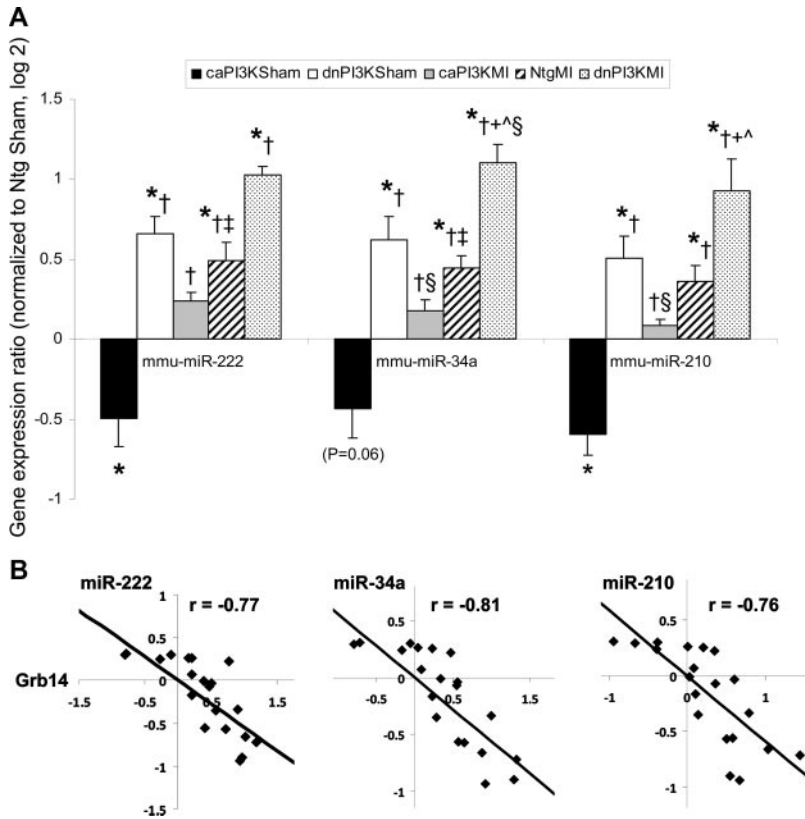


Figure 3. Differential regulation of miRNA in a setting of cardiac protection and cardiac stress. A, The miRNA decreased in a setting of cardiac protection and physiological hypertrophy (caPI3K sham) compared to Ntg sham and increased in settings of cardiac stress (Ntg MI and dnPI3K MI) compared to caPI3K MI. * $P \leq 0.05$ vs Ntg sham. † $P < 0.05$ vs caPI3K sham. ‡ $P < 0.05$ vs Ntg MI. § $P < 0.05$ vs caPI3K MI. ¶ $P < 0.05$ vs dnPI3K sham. †† $P < 0.05$ vs caPI3K MI; $P = 0.06$ vs Ntg sham $n = 4$ in each group. B, Linear correlation between Grb14 gene expression (log2) and miRNA-222, miRNA-34a, and miRNA-210 expression (log2) from the PI3K MI data set ($n = 20$; $P < 0.001$ for all correlations).

Potential Mechanisms by Which PI3K Provides Cardiac Protection

Akt is a well-characterized target of PI3K with cell survival and antiapoptotic actions in the heart.¹⁵ The phosphorylation of Akt relative to total Akt was ≈ 3.5 -fold higher in hearts of sham-operated caPI3K mice in comparison to Ntg and dnPI3K (sham and MI groups) mice and remained elevated in a setting of MI

(Figure 4A). To determine the possible physiological significance of changes in miRNA-210, we examined BDNF in our caPI3K model. BDNF is a predicted target of miRNA-210 using TargetScanMouse5.1 (based on the presence of a conserved “seed region” [nucleotides 2–7; complementary base pairing between the 3’-untranslated regions of the mRNA and the 5’ end of the miRNA]). BDNF was of added interest in the current

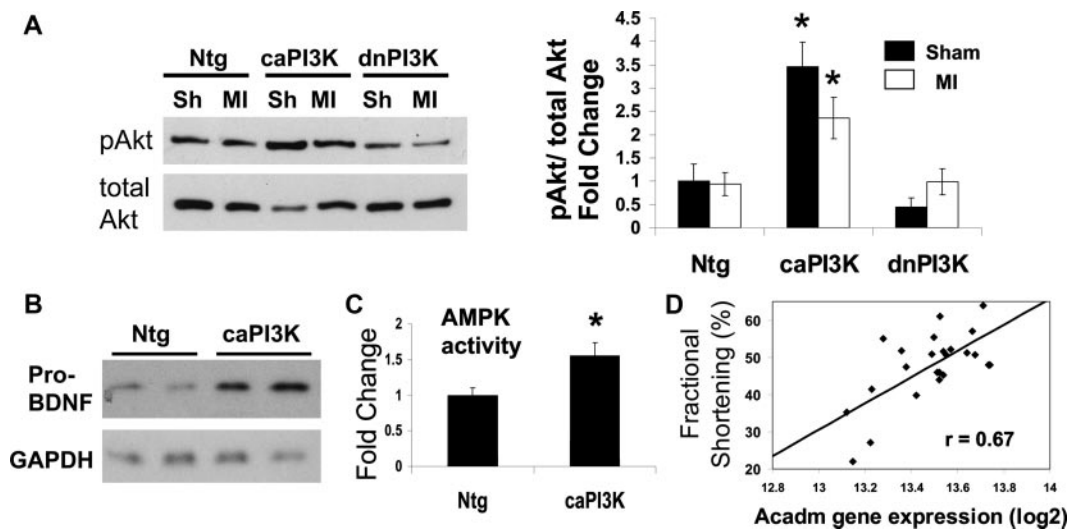


Figure 4. A, Western blot of pAkt and total Akt in hearts from Ntg, caPI3K, and dnPI3K mice subjected to sham (Sh) or MI (left). Right, Quantitative analysis of pAkt relative to total Akt. Mean values for Ntg sham were normalized to 1 (Ntg sham, $n = 7$; Ntg MI, $n = 4$; caPI3K sham, $n = 4$; caPI3K MI, $n = 3$; dnPI3K sham, $n = 4$; dnPI3K MI, $n = 4$). * $P < 0.05$ vs all Ntg and dnPI3K groups. B, Western blot of BDNF and GAPDH in isolated adult cardiac myocytes from Ntg and caPI3K mice (basal conditions). Mean values for Ntg were normalized to 1. * $P < 0.05$ vs Ntg; $n = 3$ in each group. C, AMPK activity in hearts from adult Ntg and caPI3K mice (basal conditions). Mean values for Ntg were normalized to 1. * $P < 0.05$ vs Ntg; $n = 3$ in each group. D, Correlation between medium chain acyl-Coenzyme A dehydrogenase (*Acadm*) gene expression and FS from the PI3K MI data set ($n = 24$; $P < 0.001$).

study because of a recent report demonstrating that BDNF expression is elevated in human skeletal muscle in response to exercise and that BDNF is produced by contracting skeletal muscle cells and increases fatty acid oxidation via activation of AMPK.¹⁶ BDNF protein expression was elevated in cardiac myocytes from caPI3K mice (Figure 4B), AMPK activity was increased in hearts of caPI3K mice (Figure 4C), and gene expression of *Acadm* (gene that encodes an enzyme that plays an important role in mitochondrial fatty acid oxidation in the heart) was highly correlated with FS in the PI3K MI data set (Figure 4D, Table II; $P < 0.001$).

Discussion

Atherosclerosis and its complications, including MI-induced heart failure, are increasing because of an increasing aging population and increased rates of obesity and diabetes. Current therapeutics delay heart failure progression as opposed to improving the function of the failing heart. Activation of physiological signaling cascades, such as the PI3K(p110 α) pathway, represents a novel approach that may have advantages over strategies that largely inhibit proteins that lie on pathological signaling cascades (eg, angiotensin-converting enzyme inhibitors that block the effects of angiotensin II & G-protein-coupled receptors signaling), because PI3K has the ability to mediate the cardioprotective properties of physiological hypertrophy, in addition to inhibiting proteins downstream of G-protein-coupled receptors and blunting pathological hypertrophy.¹ Consequently, this strategy may hold promise for improving function of the failing heart as opposed to simply slowing disease progression. A current challenge in targeting PI3K is related to its widespread actions and expression in multiple cell types. Whereas the current study and our previous work¹ demonstrate that activating PI3K(p110 α) in the heart is beneficial, PI3K(p110 α) also permits cancer cells to bypass normal growth-limiting controls.¹⁷ Thus, it is of great interest to identify downstream targets regulated by PI3K that may represent more specific therapeutic targets. In this study, we demonstrate that increased activity of PI3K(p110 α) can protect the heart against MI-induced heart failure, and we identify mRNA and miRNA differentially regulated by PI3K(p110 α) that are correlated with cardiac protection in a setting of cardiac stress.

By utilizing cardiac-specific Tg mouse models with increased PI3K activity (caPI3K) and decreased PI3K activity (dnPI3K), we were able to identify genes that were specifically associated with PI3K activity. Addition of the MI model allowed us to further identify mRNA that are correlated with cardiac function and are likely to play a cardioprotective role in a setting of cardiac stress. Of the 295 genes identified using this approach, there was a significant representation of genes associated with mitochondrial energy metabolism. This is not surprising given the majority of ATP generation in the healthy heart can be attributed to oxidation of fatty acids and glucose in mitochondria, and dysregulation of these processes occurs during the development of heart failure.¹⁸

One of the most interesting mRNA targets identified in the current analyses was Grb14. Grb14 mRNA expression was differentially regulated in our PI3K-Tg mouse models and was highly correlated with cardiac function in the PI3K MI data set. To directly assess the functional significance of

Grb14 in the heart, we characterized the cardiac phenotype of Grb14 KO mice. Here, we report that loss of Grb14 induces cardiomyopathy associated with an increase in heart and atrial weight, decreased cardiac function, and interstitial fibrosis. Akt activation was lower in hearts of Grb14 KO mice under basal conditions. This is consistent with reduced Akt activation in dnPI3K hearts⁸ and may explain why both animal models (ie, dnPI3K and Grb14 KO) are more susceptible to MI-induced heart failure than are control mice. The mechanism of Grb14 signaling in the heart represents an important area for further study. Known binding partners for Grb14 include the insulin receptor and fibroblast growth factor receptor-1; Grb14 negatively regulated signaling by both receptors.^{9,19} Grb14 bound to the insulin receptor in Chinese hamster ovary cells and delayed the activation of Akt,²⁰ and Grb14 inhibited Akt in cancer cells.²¹ However, we detected decreased Akt activation in Grb14 KO hearts, indicating that Grb14 exerts a positive influence on Akt activation in this tissue context. One possibility is that this reflects the interaction of Grb14 with the Akt regulator PDK1.²²

Grb14 represents an attractive regulator of the PI3K (p110 α) pathway that may be targeted in the heart because of its high expression in this organ compared with other tissues.⁹ Our findings of altered Grb14 expression in PI3K-Tg and MI hearts, together with the cardiomyopathy phenotype in the Grb14 KO mice, provide proof of principle and validation of our experimental design. The approach of identifying differentially expressed genes by microarray analysis that is correlated with a physiological outcome/end point (eg, cardiac function) represents a robust system for identifying downstream targets/regulators with functional significance.

Recently, there has been great interest in examining the therapeutic potential of miRNA in a setting of heart disease.^{23–25} The miRNA are a family of small RNA (≈ 22 nucleotides) that play important roles in the regulation of target genes by interacting/binding with specific sites in 3'-untranslated regions of messenger transcripts to repress their translation or regulate degradation.^{26,27} The miRNA are able to repress targets (proteins) with or without detectable changes in mRNA levels.²⁸ Recent studies have identified a number of miRNA linked with cardiac pathology.^{23,24} In contrast, miRNA biology of physiological cardiac hypertrophy and cardioprotection has received little attention.²⁹ One study found that miRNA-1 and miRNA-133 were decreased in 2 models of physiological cardiac hypertrophy (exercise-trained rats and cardiac-specific Akt Tg mice), but these miRNA were also decreased in a model of pathological hypertrophy (pressure overload) and in patients with heart disease.³⁰ To our knowledge, miRNA that are differentially regulated in settings of cardioprotection and cardiac stress have yet to be clearly identified. Thus, we identified miRNA differentially expressed in hearts of caPI3K and dnPI3K-Tg mice and focused on those miRNA in which expression was correlated with cardiac function in a setting of MI.

In the current study, miRNA-222, miRNA-31, miRNA-27a, miRNA-221, and miRNA-103 were all upregulated in hearts from dnPI3K sham, the noninfarcted myocardium of Ntg MI, and dnPI3K MI mice, and they have been linked with pathological hypertrophy.³¹ By contrast, each of these miRNA was downregulated in the caPI3K sham cardiac

samples, providing support for a distinct role of these miRNA in a setting of cardiac stress and cardiac protection associated with physiological hypertrophy induced by the caPI3K transgene. Van Rooij et al³² have also performed miRNA analysis in a mouse model of MI. These authors identified miRNA in the border zone of the infarcted model and noninfarcted myocardium. Whereas miRNA expression was examined at different time intervals (3 and 14 days after MI) compared to the current study (8 weeks after MI), both studies identified a number of miRNA in the noninfarcted myocardium that were upregulated (miRNA-21, miRNA-214, miRNA-222, miRNA-140*, miRNA-199a-5p, miRNA-199b).

In the current study, miRNA-222, miRNA-34a, and miRNA-210 were of interest because expression levels were decreased in our model of physiological hypertrophy (caPI3K), increased in our model with decreased PI3K activity (dnPI3K), elevated in a setting of cardiac pathology (ie, MI), and correlated with the degree of cardiac dysfunction in the MI models. These 3 miRNA were also highly correlated with Grb14 mRNA expression. Grb14 is not a predicted target of miRNA-222, miRNA-34a, or miRNA-210. However, it is recognized that almost 30% of experimentally supported miRNA-target gene interactions are not predicted by current computational miRNA target prediction programs.³³ Alternatively, these miRNA may regulate Grb14 expression via indirect effects. The high correlation of Grb14 expression with each of the miRNA together with their identification based on a correlation with cardiac function suggest important interactions may exist and will form the basis of future studies. miRNA-210 is expressed largely in heart and teeth,³⁴ is increased in failing human hearts vs healthy hearts,³⁵ and increased apoptosis in HeLa cells.³⁶ Together, this suggests that inhibition of miRNA-210 in cardiac myocytes may be beneficial. However, the role of miRNA-210 may vary in different cell types and conditions (acute vs chronic). It was recently reported that ischemic preconditioning of bone marrow-derived mesenchymal stem cells induced expression of miRNA-210 and improved cell survival via suppression of caspase-8–associated protein-2.³⁷ The preconditioned mesenchymal stem cells showed improved survival in a rat model of acute MI, and this was associated with higher miRNA-210 levels, although cardiac function was not assessed. It also remains unclear whether increased miRNA-210 expression was critical in this setting because it was not inhibited *in vivo*. Gene expression of caspase-8–associated protein-2 was not significantly altered in our study (data not shown).

Multiple miRNA are able to regulate the same targets. In the current study, semaphorin 6d was predicted to be a target of miRNA specifically regulated by PI3K, ie, miRNA-31, miRNA-221 and miRNA-222. Semaphorin 6d was shown to be required for normal embryonic cardiac development,³⁸ which is a function consistent with the role of PI3K(p110 α) mediating postnatal cardiac growth.⁸ Another semaphorin, semaphorin 4b, is a predicted target of miRNA-34a and also is differentially regulated by PI3K. Future studies will be required to directly assess the functional significance of these miRNA *in vivo* and validate the predicted mRNA targets.

To explore potential mechanisms responsible for protection provided by constitutively active PI3K in a setting of MI,

we examined the expression of a well-known target of PI3K, Akt. Akt has been linked with cardiac protection and has been shown to have antiapoptotic properties in the heart.¹⁵ It was previously reported that the phosphorylation of Akt is elevated in hearts of caPI3K-Tg mice and decreased in hearts of dnPI3K-Tg mice under basal conditions.⁸ In the current study, Akt activation was elevated in hearts from caPI3K mice under sham-operated conditions compared to Ntg sham, and it remained elevated in a setting of MI compared to all other groups. We also examined protein expression of a predicted target of miRNA-210, BDNF. BDNF protein expression was recently shown to increase in human skeletal muscle after exercise and to enhance fatty acid oxidation via an AMPK-dependent mechanism in electrically stimulated muscle cells.¹⁶ In the healthy heart, fatty acid oxidation is the main metabolic pathway responsible for generating energy,³⁹ and it increases in response to exercise.⁴⁰ By contrast, fatty acid oxidation decreases in a setting of pathological hypertrophy, cardiac stress, and heart failure.^{41,42} In the current study, BDNF protein expression was increased in cardiac myocytes from caPI3K mice (miRNA-210 expression decreased in this setting; caPI3K sham), activation of AMPK was elevated in hearts of caPI3K mice, and gene expression of a key enzyme for fatty acid oxidation in the heart (medium chain acyl-Coenzyme A dehydrogenase; previously shown to be elevated in caPI3K hearts⁴³) was highly correlated with cardiac function in the current PI3K MI study. Together, this suggests that increased PI3K activity might protect the heart against dysfunction after chronic MI by maintaining fatty acid oxidation and Akt activation in the heart.

Here, we identify a set of miRNA and mRNA that are specifically regulated by PI3K(p110 α) and that are associated with a cardioprotective phenotype. We have validated our experimental approach by demonstrating that loss of a protein associated with the cardioprotective phenotype of caPI3K, ie, Grb14, leads to cardiac dysfunction under basal conditions and after MI. Grb14 represents a promising new target for the treatment of heart failure because of its high expression in the heart compared with other tissues. The miRNA or direct targets that mediate the protective properties of PI3K(p110 α) selectively in the myocardium have the potential to restore function to the failing heart and represent attractive therapeutic targets that would be better-tolerated in patients than activating PI3K(p110 α) directly.

Sources of Funding

This study was funded by National Health and Medical Research Council Project grants 367600 and 526647, and a Ramaciotti Establishment grant (to J.R.M.). J.R.M. was supported by a Career Development Award cofunded by the National Health and Medical Research Council and National Heart Foundation of Australia. J.R.M. is supported by an Australian Research Council Future Fellowship. V.B.M. is supported by a National Health and Medical Research Council Career Development Award. R.C.Y.L. and R.B.H.W. were supported by National Health and Medical Research Council Peter Doherty Fellowships. J.R.M., E.A.W., R.J.D., M.A.F., and X.J.D. are National Health and Medical Research Council fellows.

Disclosures

None.

References

- McMullen JR, Amirahmadi F, Woodcock EA, Schinke-Braun M, Bouwman RD, Hewitt KA, Mollica JP, Zhang L, Zhang Y, Shioi T, Bueger A, Izumo S, Jay PY, Jennings GL. Protective effects of exercise and phosphoinositide 3-kinase(p110alpha) signaling in dilated and hypertrophic cardiomyopathy. *Proc Natl Acad Sci U S A*. 2007;104:612–617.
- McMullen JR, Shioi T, Huang W-Y, Zhang L, Tarnavski O, Bisping E, Schinke M, Kong S, Sherwood MC, Brown J, Riggi L, Kang PM, Izumo S. The insulin-like growth factor 1 receptor induces physiological heart growth via the phosphoinositide 3-kinase(p110alpha) pathway. *J Biol Chem*. 2004;279:4782–4793.
- McMullen JR, Shioi T, Zhang L, Tarnavski O, Sherwood MC, Kang PM, Izumo S. Phosphoinositide 3-kinase(p110alpha) plays a critical role for the induction of physiological, but not pathological, cardiac hypertrophy. *Proc Natl Acad Sci U S A*. 2003;100:12355–12360.
- Levy D, Garrison RJ, Savage DD, Kannel WB, Castelli WP. Prognostic implications of echocardiographically determined left ventricular mass in the Framingham Heart Study. *N Engl J Med*. 1990;322:1561–1566.
- Cohn JN, Bristow MR, Chien KR, Colucci WS, Frazier OH, Leinwand LA, Lorell BH, Moss AJ, Sonnenblick EH, Walsh RA, Mockrin SC, Reinlib L. Report of the National Heart, Lung, and Blood Institute Special Emphasis Panel on Heart Failure Research. *Circulation*. 1997;95:766–770.
- McMullen JR, Jennings GL. Differences between pathological and physiological cardiac hypertrophy: novel therapeutic strategies to treat heart failure. *Clin Exp Pharmacol Physiol*. 2007;34:255–262.
- McMullen JR. Role of insulin-like growth factor 1 and phosphoinositide 3-kinase in a setting of heart disease. *Clin Exp Pharmacol Physiol*. 2008;35:349–354.
- Shioi T, Kang PM, Douglas PS, Hampe J, Yballe CM, Lawitts J, Cantley LC, Izumo S. The conserved phosphoinositide 3-kinase pathway determines heart size in mice. *EMBO J*. 2000;19:2537–2548.
- Cooney GJ, Lyons RJ, Crew AJ, Jensen TE, Molero JC, Mitchell CJ, Biden TJ, Ormandy CJ, James DE, Daly RJ. Improved glucose homeostasis and enhanced insulin signalling in Grb14-deficient mice. *EMBO J*. 2004;23:582–593.
- Tarnavski O, McMullen JR, Schinke M, Nie Q, Kong S, Izumo S. Mouse cardiac surgery: comprehensive techniques for the generation of mouse models of human diseases and their application for genomic studies. *Physiol Genomics*. 2004;16:349–360.
- Gao XM, Xu Q, Kiriazis H, Dart AM, Du XJ. Mouse model of post-infarct ventricular rupture: time course, strain- and gender-dependency, tensile strength, and histopathology. *Cardiovasc Res*. 2005;65:469–477.
- Du XJ, Autelitano DJ, Dilley RJ, Wang B, Dart AM, Woodcock EA. Beta(2)-adrenergic receptor overexpression exacerbates development of heart failure after aortic stenosis. *Circulation*. 2000;101:71–77.
- Shioi T, McMullen JR, Kang PM, Douglas PS, Obata T, Franke TF, Cantley LC, Izumo S. Akt/protein kinase B promotes organ growth in transgenic mice. *Mol Cell Biol*. 2002;22:2799–2809.
- Steinberg GR, Smith AC, Van Denderen BJ, Chen Z, Murthy S, Campbell DJ, Heigenhauser GJ, Dyck DJ, Kemp BE. AMP-activated protein kinase is not down-regulated in human skeletal muscle of obese females. *J Clin Endocrinol Metab*. 2004;89:4575–4580.
- Matsui T, Nagoshi T, Rosenzweig A. Akt and PI 3-kinase signaling in cardiomyocyte hypertrophy and survival. *Cell Cycle*. 2003;2:220–223.
- Matthews VB, Astrom MB, Chan MH, Bruce CR, Krabbe KS, Prelovsek O, Akerstrom T, Yfanti C, Broholm C, Mortensen OH, Penkowa M, Hojman P, Zankari A, Watt MJ, Bruunsgaard H, Pedersen BK, Febbraio MA. Brain-derived neurotrophic factor is produced by skeletal muscle cells in response to contraction and enhances fat oxidation via activation of AMP-activated protein kinase. *Diabetologia*. 2009;52:1409–1418.
- McMullen JR, Jay PY. PI3K(p110alpha) Inhibitors as anti-cancer agents: minding the heart. *Cell Cycle*. 2007;6:910–913.
- Huss JM, Kelly DP. Mitochondrial energy metabolism in heart failure: a question of balance. *J Clin Invest*. 2005;115:547–555.
- Reilly JF, Mickey G, Maher PA. Association of fibroblast growth factor receptor 1 with the adaptor protein Grb14. Characterization of a new receptor binding partner. *J Biol Chem*. 2000;275:7771–7778.
- Berezziat V, Kasus-Jacobi A, Perdereau D, Cariou B, Girard J, Burnol AF. Inhibition of insulin receptor catalytic activity by the molecular adapter Grb14. *J Biol Chem*. 2002;277:4845–4852.
- Caillaud K, Perdereau D, Lescuyer A, Chen H, Garbay C, Vilain JP, Burnol AF, Browaeys-Poly E. FGF receptor phosphotyrosine 766 is a target for Grb14 to inhibit MDA-MB-231 human breast cancer cell signaling. *Anticancer Res*. 2005;25:3877–3882.
- King CC, Newton AC. The adaptor protein Grb14 regulates the localization of 3-phosphoinositide-dependent kinase-1. *J Biol Chem*. 2004;279:37518–37527.
- Divakaran V, Mann DL. The emerging role of microRNA in cardiac remodeling and heart failure. *Circ Res*. 2008;103:1072–1083.
- van Rooij E, Sutherland LB, Liu N, Williams AH, McAnally J, Gerard RD, Richardson JA, Olson EN. A signature pattern of stress-responsive microRNA that can evoke cardiac hypertrophy and heart failure. *Proc Natl Acad Sci U S A*. 2006;103:18255–18260.
- van Rooij E, Olson EN. MicroRNA: powerful new regulators of heart disease and provocative therapeutic targets. *J Clin Invest*. 2007;117:2369–2376.
- Griffiths-Jones S, Grocock RJ, van Dongen S, Bateman A, Enright AJ. miRBase: microRNA sequences, targets and gene nomenclature. *Nucleic Acids Res*. 2006;34:D140–D144.
- Bartel DP. MicroRNA: genomics, biogenesis, mechanism, and function. *Cell*. 2004;116:281–297.
- Baek D, Villen J, Shin C, Camargo FD, Gygi SP, Bartel DP. The impact of microRNA on protein output. *Nature*. 2008;455:64–71.
- Latronico MV, Catalucci D, Condorelli G. MicroRNA and cardiac pathologies. *Physiol Genomics*. 2008;34:239–242.
- Care A, Catalucci D, Felicetti F, Bonci D, Addario A, Gallo P, Bang ML, Segnalini P, Gu Y, Dalton ND, Elia L, Latronico MV, Hoydal M, Autore C, Russo MA, Dorn GW II, Ellingsen O, Ruiz-Lozano P, Peterson KL, Croce CM, Peschle C, Condorelli G. MicroRNA-133 controls cardiac hypertrophy. *Nat Med*. 2007;13:613–618.
- Sayed D, Hong C, Chen IY, Lypowy J, Abdellatif M. MicroRNA play an essential role in the development of cardiac hypertrophy. *Circ Res*. 2007;100:416–424.
- van Rooij E, Sutherland LB, Thatcher JE, DiMaio JM, Naseem RH, Marshall WS, Hill JA, Olson EN. Dysregulation of microRNA after myocardial infarction reveals a role of miR-29 in cardiac fibrosis. *Proc Natl Acad Sci U S A*. 2008;105:13027–13032.
- Sethupathy P, Megraw M, Hatzigeorgiou AG. A guide through present computational approaches for the identification of mammalian microRNA targets. *Nat Methods*. 2006;3:881–886.
- Babak T, Zhang W, Morris Q, Blencowe BJ, Hughes TR. Probing microRNA with microarrays: tissue specificity and functional inference. *RNA*. 2004;10:1813–1819.
- Thum T, Galuppo P, Wolf C, Fiedler J, Kneitz S, van Laake LW, Doevendans PA, Mummery CL, Borlak J, Haverich A, Gross C, Engelhardt S, Ertl G, Bauersachs J. MicroRNA in the human heart: a clue to fetal gene reprogramming in heart failure. *Circulation*. 2007;116:258–267.
- Cheng AM, Byrom MW, Shelton J, Ford LP. Antisense inhibition of human miRNA and indications for an involvement of miRNA in cell growth and apoptosis. *Nucleic Acids Res*. 2005;33:1290–1297.
- Won Kim H, Haider HK, Jiang S, Ashraf M. Ischemic preconditioning augments survival of stem cells via miR-210 expression by targeting caspase-8-associated protein 2. *J Biol Chem*. 2009;284:33161–33168.
- Toyofuku T, Zhang H, Kumanogoh A, Takegahara N, Suto F, Kamei J, Aoki K, Yabuki M, Hori M, Fujisawa H, Kikutani H. Dual roles of Sema6D in cardiac morphogenesis through region-specific association of its receptor, Plexin-A1, with off-track and vascular endothelial growth factor receptor type 2. *Genes Dev*. 2004;18:435–447.
- van der Vusse GJ, Glatz JF, Stam HC, Reneman RS. Fatty acid homeostasis in the normoxic and ischemic heart. *Physiol Rev*. 1992;72:881–940.
- Gertz EW, Wisneski JA, Stanley WC, Neese RA. Myocardial substrate utilization during exercise in humans. Dual carbon-labeled carbohydrate isotope experiments. *J Clin Invest*. 1988;82:2017–2025.
- Allard MF, Schonekess BO, Henning SL, English DR, Lopaschuk GD. Contribution of oxidative metabolism and glycolysis to ATP production in hypertrophied hearts. *Am J Physiol*. 1994;267:H742–H750.
- Davila-Roman VG, Vedala G, Herrero P, de las Fuentes L, Rogers JG, Kelly DP, Gropler RJ. Altered myocardial fatty acid and glucose metabolism in idiopathic dilated cardiomyopathy. *J Am Coll Cardiol*. 2002;40:271–277.
- O'Neill BT, Kim J, Wende AR, Theobald HA, Tuinei J, Buchanan J, Guo A, Zaha VG, Davis DK, Schell JC, Boudina S, Wayment B, Litwin SE, Shioi T, Izumo S, Birnbaum MJ, Abel ED. A conserved role for phosphatidylinositol 3-kinase but not Akt signaling in mitochondrial adaptations that accompany physiological cardiac hypertrophy. *Cell Metab*. 2007;6:294–306.